Functional Split-Aware Design of Power-over-Fiber 6G O-RAN Fronthaul Networks

Luiz G. S. Dos Santos[1], Egemen Erbayat[2], Suresh Subramaniam[2], Gustavo B. Figueiredo[1]
[1]*Federal University of Bahia*, [2]*The George Washington University*

***Abstract*—Forthcoming 6G networks impose stringent requirements on fronthaul capacity, latency, and energy efficiency, particularly under disaggregated Open Radio Access Network (O-RAN) architectures. Power-over-Fiber (PWoF) technology offers a viable transport solution by enabling the joint delivery of data and power over optical infrastructure. This paper addresses the problem of designing PWoF-enabled fronthaul networks under different functional split (FS) options. We formulate a mixed-integer linear programming (MILP) model to minimize the total cost of ownership (TCO) while guaranteeing feasibility for a given set of FS configurations. Numerical results show that the proposed model computes optimal solutions even for large-scale networks and underline the impact of FS on fronthaul cost and resource utilization. These findings highlight the importance of split-aware fronthaul planning for future 6G networks.**

***Index Terms*—Power over Fiber, Fronthaul Networks, Functional Split, Optimization, O-RAN**

I. Introduction

The rapid evolution toward 6G mobile networks is driven by the need to support ultra-high data rates, projected to reach peak data rates of up to 1 Tbps, and extremely low-latency communication [1]. To support this new generation of networks, the industry is transitioning toward Open Radio Access Network (O-RAN) architectures. Unlike traditional RAN deployments, O-RAN emphasizes openness and flexibility, fostering innovation and reducing vendor lock-in in the 6G era. A key challenge of this paradigm is the growing demand for high-capacity, cost-efficient fronthaul infrastructure to connect the Open Distributed Units (O-DUs) to the Open Remote Units (O-RUs). To meet these requirements, Time and Wavelength Division Multiplexed Passive Optical Networks (TWDM-PON) can be leveraged for the transport network to support multiple virtual point-to-multipoint links over a shared fiber infrastructure. Another critical challenge in fronthaul design is the efficient and reliable provisioning of electrical power to the O-RUs. Recently, the Power-over-Fiber (PWoF) technology has emerged as a promising solution that enables the simultaneous transmission of electrical power and data over optical fibers [2].

However, integrating PWoF into O-RAN fronthaul networks requires solving complex optimization problems to minimize the total cost of ownership (TCO). Several recent studies have addressed this challenge. In [3], the authors consider deployment scenarios with a single DU and multiple splitters, demonstrating that the multi-splitter assignment problem is NP-hard and formulating it as an Integer Linear Programming (ILP) model. Subsequently, [4] proposed the Randomized Successive Splitter Assignment (RSSA) heuristic for multi-DU scenarios, while [5] incorporated latency constraints and introduced the Meta K-Means Clustering Boosting (MKMC) heuristic. Finally, [6] investigates survivable network design under fiber and node failure scenarios. Although these studies represent a significant advancement in fronthaul planning, they do not explicitly account for functional split requirements, particularly in terms of bandwidth constraints and distributed processing demands.

Functional Splitting (FS) refers to the partitioning of RAN protocol stack functions across multiple physical and/or logical entities. O-RAN supports multiple FS options between O-RUs, O-DUs, and Open Central Units (O-CUs), which host centralized processing functions (PFs) with distinct transport and computational requirements. These functions are typically implemented as Virtualized Network Functions (VNFs) deployed on general-purpose hardware. The choice of FS is a critical design decision, as it directly determines the bandwidth and latency requirements of the transport links, as well as the computational load at each processing node. Previous studies have considered FS requirements in fronthaul network planning [7], [8]. However, these studies do not jointly consider multiple FS options or the impact of VNF processing requirements on deployment and operational costs. To address this gap, in this paper, we propose a Mixed-Integer Linear Programming (MILP) formulation for fronthaul network design that jointly incorporates PWoF technology and multi-option FS awareness. The proposed model aims to minimize the TCO of the network deployment while enabling the operation of any FS given as input during production. The remainder of this paper is organized as follows. Section **II** describes the network architecture. Section **III** formulates the optimization problem, and Section **IV** presents the MILP formulation. Section **V** evaluates the proposed approach and Section **VI** concludes the paper.

II. Network Architecture and Functional Split Model

A. Network Architecture

We propose an O-RAN architecture that leverages a power-enabled optical network as its transport network. In O-RAN, the RAN protocol stack and processing functions are disaggregated into three logical components: O-CU, O-DU, and the O-RU. For convenience, these entities are hereafter referred to as CU, DU, and RU, respectively. These units are deployed across different network locations. In the considered scenario, the RU is always located at the cell site, while the DU and CU are deployed at edge nodes and a centralized cloud node, respectively. The RU interfaces with the DU through the fronthaul, whereas the DU interfaces with the CU via the midhaul. Each logical component may host a different number

978-3-903176-78-2 © 2026 IFIP

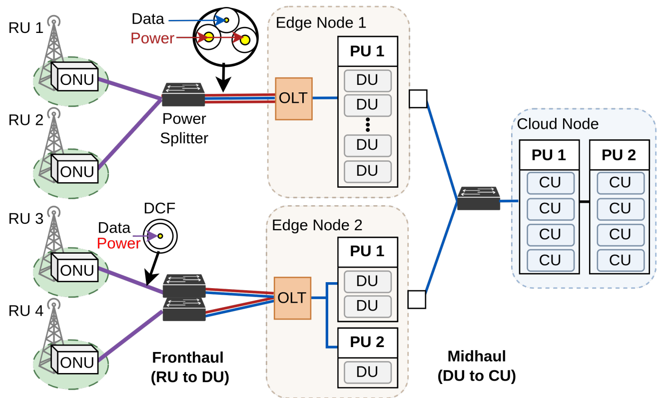

Fig. 1: PWoF-enabled PON fronthaul architecture.

of VNFs depending on the adopted FS. The FS determines how RAN functions are distributed among RU, DU, and CU, and can be dynamically configured by the operator to meet Quality of Service (QoS) requirements while adapting to available transport and processing resources.

The underlying optical transport network is based on a TWDM-PON, as illustrated in Fig. 1. The TWDM-PON comprises Optical Line Terminals (OLTs) deployed at the edge nodes, and Optical Network Units (ONUs) located at the cell sites. In addition to these entities, passive optical splitters are used to aggregate traffic from multiple ONUs toward an OLT. To support both data transmission and energy delivery, the network utilizes PWoF technology for the fronthaul. In particular, the connections between OLTs and splitters employ fiber bundles composed of single-mode (SM) and multimode (MM) cores. The SM core is used for data transmission, while each MM core is dedicated to delivering optical power to an RU. With the current state of PWoF technology, up to four RUs can be powered by a single fiber bundle. Furthermore, double-clad fibers (DCFs) are used to connect splitters to ONUs, enabling the simultaneous transmission of data and power over a single fiber. In addition, SM fibers are used to connect the cloud node to the edge nodes. It should be noted that existing DCF coupler technology restricts the maximum input power from the splitter to each DCF to 20 W [9].

B. Functional Split Model

The FS model adopted in this work is based on [10]–[12]. The RAN protocol stack is decomposed into eight processing functions (PF_1 to PF_8), each implemented as a VNF. The placement of these functions depends on the selected FS, which determines whether a function is executed at the RU, DU, or CU. Specifically, Split Option 2 centralizes PF_1 (PDCP), Option 4 additionally centralizes PF_2 (RLC), and Option 6 includes PF_3 (MAC). Split 7a further centralizes PF_4 (FEC). O-RAN Split 7-2x divides the physical layer by centralizing modulation, scrambling, and layer mapping functions (PF_5^{High}), while retaining precoding and beamforming (PF_5^{Low}) at the RU. Lower-level splits, such as 7b and 7c, progressively centralize the remaining PHY functions up to full OFDM grid generation (PF_6).

The processing cost of each function, expressed in Giga perations per second (GOPS), depends on the traffic load $\rho \in [0, 1]$, the number of antennas A, the number of spatial layers L, and the system bandwidth B. Reference processing costs are denoted by $G_{\text{Ref}}^{\text{Fx}}$, and the resulting processing requirements are computed as follows:

$$PF_1(\text{PDCP}) = G_{\text{Ref}}^{\text{PDCP}} \cdot \rho \cdot \frac{A}{A_{\text{Ref}}}$$

$$PF_2(\text{RLC}) = G_{\text{Ref}}^{\text{RLC}} \cdot \rho \cdot \frac{A}{A_{\text{Ref}}}$$

$$PF_3(\text{MAC}) = G_{\text{Ref}}^{\text{MAC}} \cdot \rho \cdot \frac{A}{A_{\text{Ref}}}$$

$$PF_4(\text{FEC}) = G_{\text{Ref}}^{\text{FEC}} \cdot \rho \cdot \frac{B}{B_{\text{Ref}}}$$

$$PF_5^{\text{High}}(\text{Mod/LayerMap}) = G_{\text{Ref}}^{\text{Mod}} \cdot \rho \cdot \frac{B}{B_{\text{Ref}}} \cdot L$$

$$PF_5^{\text{Low}}(\text{Precoding}) = G_{\text{Ref}}^{\text{Pre}} \cdot \rho \cdot \frac{B}{B_{\text{Ref}}} \cdot \frac{A}{A_{\text{Ref}}}$$

$$PF_6(\text{RE Mapping}) = G_{\text{Ref}}^{\text{Map}} \cdot \rho \cdot \frac{B}{B_{\text{Ref}}} \cdot \frac{A}{A_{\text{Ref}}}$$

$$PF_7(\text{OFDM}) = G_{\text{Ref}}^{\text{OFDM}} \cdot \frac{B}{B_{\text{Ref}}} \cdot \frac{A}{A_{\text{Ref}}}$$

$$PF_8(\text{RF}) = G_{\text{Ref}}^{RF} \cdot \frac{B}{B_{\text{Ref}}} \cdot \frac{A}{A_{\text{Ref}}}$$

Furthermore, the bandwidth requirements associated with each FS are derived from the traffic load, protocol overheads, and physical layer parameters. The user-plane throughput R_{user} scales linearly with the ρ. For physical-layer splits, the required bandwidth depends on either the number of active resource blocks ($N_{\text{PRB}}^{\text{act}}$) or the total system bandwidth (N_{PRB}^{t}). The bit widths for frequency-domain IQ samples, time-domain IQ samples, and soft bits are denoted by N_{IQ}, N_{CPRI}, and N_{LLR}, respectively. Additional parameters include the number of subcarriers per resource block (N_{SC}), the number of OFDM symbols per subframe (N_{sym}), and protocol-specific overhead factors Ω_{IP}, Ω_{PDCP}, Ω_{RLC}, Ω_{FAPI}, and Ω_{eCPRI}. Table I summarizes the bandwidth expressions and maximum one-way latency constraints for the considered 3GPP and O-RAN FS.

III. Problem Statement

This section formally defines the fronthaul network design problem. The formulation builds upon prior PWoF-enabled fronthaul optimization studies [3]–[6] by explicitly incorporating bandwidth, latency, and processing constraints induced by FS. Following the architecture described in Section II, RUs are deployed at cell sites and are co-located with ONUs. For simplicity, each RU–ONU pair is henceforth referred to as an RU. Accordingly, the problem takes as input the geographical positions of already deployed RUs, as well as a set of candidate splitter locations, a set of candidate edge node locations, a single cloud node location, and a predefined set of FS options. Moreover, each RU must be connected to an edge node through a splitter, while each splitter location may host multiple deployed splitters.

TABLE I: Bandwidth and Latency Requirements for Functional Splits.

Split	Bandwidth Calculation	Latency
1	$R_{\text{user}} \cdot \Omega_{\text{IP}}$	10 ms
2	$R_{\text{user}} \cdot \Omega_{\text{PDCP}}$	10 ms
4	$R_{\text{user}} \cdot \Omega_{\text{RLC}}$	100 μs
6	$R_{\text{user}} \cdot \Omega_{FAPI}$	250 μs
7a	$N_{\text{PRB}}^{\text{act}} \cdot N_{\text{SC}} \cdot N_{\text{sym}} \cdot Q_m \cdot L \cdot N_{\text{LLR}} \cdot 10^{-3}$	250 μs
7-2x	$N_{\text{PRB}}^{\text{act}} \cdot N_{\text{SC}} \cdot N_{\text{sym}} \cdot N_{\text{IQ}} \cdot L \cdot \Omega_{\text{eCPRI}} \cdot 10^{-3}$	250 μs
7b	$N_{\text{PRB}}^{\text{act}} \cdot N_{\text{SC}} \cdot N_{\text{sym}} \cdot N_{\text{IQ}} \cdot A \cdot \Omega_{\text{eCPRI}} \cdot 10^{-3}$	250 μs
7c	$N_{\text{PRB}}^{t} \cdot N_{\text{SC}} \cdot N_{\text{sym}} \cdot N_{\text{IQ}} \cdot A \cdot \Omega_{\text{eCPRI}} \cdot 10^{-3}$	250 μs
8	$f_s \cdot N_{\text{CPRI}} \cdot A \cdot \frac{10}{8} \cdot 10^{-6}$	250 μs

The design objective accounts for the cost of these connections, as well as the cost of connecting edge nodes to the cloud node. Traffic generated by each RU is modeled over a set of discrete time slots, each representing a subdivision of the operational day. This traffic load factors in determining the bandwidth and processing requirements associated with each FS option. Each FS is defined by a pair of RU-DU and DU-CU split choices. At each selected edge node, a limited number of Processing Units (PUs) can be deployed to host DU-related VNFs. The cloud node is assumed to have a predefined number of available PUs, which can be activated as needed to satisfy the aggregated processing demands of the CU-related functions.

Therefore, the goal of the problem is to determine: (i) the splitter locations and the number of deployed splitters, (ii) the selected edge node locations, (iii) the number of activated PUs at edge and cloud nodes, and (iv) the assignment of RUs to edge nodes through splitters, such that all PWoF, bandwidth, latency, and processing constraints imposed by the given FS options are satisfied, while minimizing the TCO of the network.

IV. MILP Formulation

This section presents the MILP formulation for the fronthaul network optimization problem. Given the positions of RUs, candidate splitter locations, and candidate edge node locations, the goal is to design a cost-efficient fronthaul network by assigning each RU to an edge node via a splitter, while ensuring that the resulting network can operate under any FS option provided as input.

We emphasize that the proposed formulation does not aim to optimize the selection of FS options. This design choice is motivated by the inherent uncertainty of traffic projections during the planning phase and the ability of O-RAN systems to dynamically reconfigure FS during operation. In this manner, the proposed model provides flexibility for online configuration rather than optimizing for a static split choice.

The objective is to minimize the TCO of the network. This includes fiber and trenching costs, device deployment costs (splitters and processing units), and operational energy costs. RU costs are not considered. Fiber costs depend on the unit-length costs of MM, SM, and DCF, while energy costs account for power losses along fibers and processing-related power consumption at the chosen nodes. For simplicity, we do not consider connector and splitter insertion losses, nor photovoltaic conversion efficiency at the ONU side.

A. Sets and Parameters

- $\mathcal{R}$: Set of RUs,
- $\mathcal{S}$: Set of candidate splitter positions,
- $\mathcal{E}$: Set of candidate edge node positions,
- C: Cloud node position,
- $\mathcal{N} = \mathcal{E} \cup C$: Set of processing nodes positions,
- $\mathcal{F}$: Set of functional splits,
- $\mathcal{T}$: Set of discrete time slots,
- c_{rft}^{DU}, c_{rft}^{CU}: DU and CU processing demand in GOPS of RU r under split f at time t,
- b_{rft}^{FH}, b_{rft}^{MH}: Fronthaul and midhaul bandwidth demand for RU r, split f, at time t,
- α_f^{FH}, α_f^{MH}: Maximum allowable fronthaul and midhaul propagation delay for split f,
- K: Processing capacity of a PU,
- $\mathcal{N}_{\max}^{n}$: Maximum number of activated PUs at position n
- L_{je}: Capacity of the fronthaul link from candidate splitter location j to candidate edge node location e,
- L_e: Capacity of the midhaul link from edge node e to the cloud node,
- γ: Bandwidth aggregation factor,
- $s_p^{\max}$: Maximum splitting ratio,
- χ: Fiber propagation delay per unit length,
- $d^{e_i s_j}$: Distance from edge node e to splitter j,
- $d^{s_j r_k}$: Distance from splitter j to RU r,
- $d^{e_i C}$: Distance from edge node e to the cloud node,
- $P_{\max}^{\text{dcf}}$: Maximum power supplied by a splitter for each DCF,
- η: Trenching cost per meter,
- $\zeta^{\text{mm}}, \zeta^{\text{sm}}, \zeta^{\text{dcf}}$: Cost per unit length for MM, SM, and DCF,
- $\gamma^{\text{mm}}, \gamma^{\text{dcf}}$: Power loss per unit length for MM and DCF,
- C_{PU}, C_S: Cost of a PU and a splitter,
- β: Power generation cost per watt/year,
- τ: Expected operating time (years),
- H_{sn}: Static (idle) power consumption of node n in Watts,
- H_{dn}: Dynamic power coefficient of node n in W/GOPS, representing the additional power consumption per unit of processing load.

B. Decision Variables

- $\sigma_e \in \{0,1\}$: 1 if edge location e is selected,
- $\delta_{ej} \in \{0,1\}$: 1 if candidate edge location e is connected to candidate splitter location j,
- ξ_{ej}: Number of splitters installed at candidate position j for candidate edge node position e,
- $\psi_{ejr} \in \{0,1\}$: 1 if RU r connects to candidate edge node location e via candidate splitter j,
- υ_n: Number of activated PUs at node position $n \in \mathcal{N}$.

- $p_{re}^{DU} \in \{0,1\}$: 1 if DU for RU r for all split options is placed at edge node location e.

C. Constraints

$$\sum_{e\in\mathcal{E}}\sum_{j\in\mathcal{S}}\psi_{ejr} = 1, \qquad \forall r \qquad (1)$$

$$\sum_{r\in\mathcal{R}}\psi_{ejr} \le s_p^{\max}\cdot\xi_{ej}, \qquad \forall e,j \qquad (2)$$

$$\sum_{r\in\mathcal{R}}\psi_{ejr} \ge \delta_{ej}, \qquad \forall e,j \qquad (3)$$

$$\psi_{ejr} \le \delta_{ej}, \qquad \forall e,j,r \qquad (4)$$

$$\sum_{j\in\mathcal{S}}\delta_{ej} \ge \sigma_e, \qquad \forall e \qquad (5)$$

$$\delta_{ej} \le \sigma_e, \qquad \forall e,j \qquad (6)$$

$$10^{\frac{d^{s_j r_k}\gamma^{\text{dcf}}}{10}} P_k^R \psi_{i,j,k} \le P_{\max}^{\text{dcf}}, \qquad \forall i,j,k \qquad (7)$$

Constraint (1) ensures that each RU is connected to only one edge node through a splitter. Constraint (2) determines that the number of RUs assigned to a splitter is limited by its splitting ratio. Constraints (3) and (4) state that a splitter position is only chosen if it has at least one RU connected to it. Constraint (5) and (6) guarantee that an edge node location is selected if and only if it is connected to a splitter. Finally, constraint (7) ensures that each DCF fiber provides sufficient power for each RU taking into account power losses.

$$p_{re}^{DU} = \sum_{j\in\mathcal{S}}\psi_{ejr}, \qquad \forall r,e \qquad (8)$$

Constraint (8) ensures that the DU function for every split f is hosted on the specific edge node where the RU is connected.

$$\sum_{r\in\mathcal{R}}(c_{rft}^{DU}\cdot p_{re}^{DU}) \le K\cdot\upsilon_e, \qquad \forall e,f,t \qquad (9)$$

$$\sum_{r\in\mathcal{R}} c_{rft}^{CU} \le K\cdot\upsilon_c, \qquad \forall f,t \qquad (10)$$

Constraints (9) and (10) state that the total amount of operations per second assigned to a node must be less than its processing capacity.

$$\gamma\sum_{r\in\mathcal{R}}(b_{rtf}^{FH}\cdot\psi_{ejr}) \le L_{je}\cdot\xi_{ej}, \qquad \forall e,j,f,t \qquad (11)$$

$$\gamma\sum_{r\in\mathcal{R}}(b_{rtf}^{MH}\cdot p_{re}^{DU}) \le L_e, \qquad \forall e,f,t \qquad (12)$$

Constraint (11) asserts that the capacity of a link connecting a splitter to an edge node must be greater than the sum of the bandwidth demands of the RUs assigned to the splitter at any time, adjusted by the aggregation factor. Constraint (12) states that the total traffic, adjusted by the aggregation factor, passing through a link that connects an edge node to the cloud node must be less than its capacity at any time.

$$\upsilon_n \le \mathcal{N}_{\max}^n, \qquad \forall n. \qquad (13)$$

Constraint (13) states that the number of activated PUs per node location is limited by a threshold.

$$\psi_{ijk}\cdot(d^{e_i s_j} + d^{s_j r_k})\cdot\chi \le \alpha_f^{FH}, \qquad \forall i,j,k,f \qquad (14)$$

$$p_{ri}^{DU}\cdot d^{e_i C}\cdot\chi \le \alpha_f^{MH}. \qquad \forall r,i,f \qquad (15)$$

Constraints (14) and (15) state the maximum propagation delay allowed for the fronthaul and midhaul segment, respectively.

D. Cost Calculations

1) Fiber cost:

$$F_p = \sum_{i,j} d^{e_i s_j}\zeta^{\text{sm}}\xi_{ij} + \sum_{i,j,k}\psi_{ijk}(d^{e_i s_j}\zeta^{\text{mm}} + d^{s_j r_k}\zeta^{\text{dcf}}) + \sum_i d^{e_i C}\cdot\zeta^{\text{sm}}\cdot\sigma_i \qquad (16)$$

2) Trenching cost:

$$F_t = \sum_{i,j}\delta_{ij}\cdot d^{e_i s_j}\cdot\eta + \sum_{i,j,r}\psi_{ijk}\cdot d^{s_j r_k}\cdot\eta + \sum_i d^{e_i C}\cdot\eta\cdot\sigma_i \qquad (17)$$

3) Devices Cost:

$$C_D = \sum_{e\in\mathcal{E}} C_{PU}\cdot\upsilon_e + \sum_{e,j}\xi_{ej}\cdot C_S \qquad (18)$$

4) Power cost:

$$P = \sum_{i,j,k}\psi_{ijk}\cdot 10^{\frac{d^{e_i s_j}\gamma_{mmf} + d^{s_j r_k}\gamma_{dcf}}{10}}\cdot P_k^R \qquad (19)$$

The power cost model also accounts for both static and load-dependent processing power at active nodes, as well as power losses in fiber-based power delivery. To ensure worst-case operability across time, the peak processing load is considered when estimating operational energy costs

$$H_s = \sum_{n\in\mathcal{N}} H_{sn}\cdot\upsilon_n \qquad (20)$$

To calculate the dynamic energy consumption H_d, we take the peak processing power required across all time slots, considering the most demanding split option for each RU. For this, we add two additional variables k_n, representing the peak load of node n, and x_{rnt}, representing the peak load for RU r at node n and time t. Finally, H_d is calculated with the following constraints:

$$x_{ret} \ge c_{rft}^{DU}\cdot p_{re}^{DU}\cdot H_{de} \qquad \forall r,e,t,f \qquad (21)$$

$$x_{rct} \ge c_{rft}^{CU}\cdot H_{dc} \qquad \forall r,t,f \qquad (22)$$

$$k_n \ge \sum_{r\in R} x_{rnt} \qquad \forall n,t \qquad (23)$$

$$H_d = \sum_{n\in N} k_n \qquad (24)$$

TABLE II: Network and Functional Split Parameters

Parameter	Value
L_{je}, L_e	25 Gb/s, 600 Gb/s
ζ^{mm}, ζ^{smf}, ζ^{dcf}	6000, 4000, 12000 \$/km
η	16000 \$/km
γ^{mm}, γ^{dcf}	1, 1.46 dB/km
$P^{\text{dcf}}_{\max}$	20 W
χ_{fiber}	5 μs/km
K	28800 GOPS [10]
$\mathcal{N}^{\text{e}}_{\max}$, $\mathcal{N}^{\text{c}}_{\max}$	300, 500
H_{sn}, H_{dn}	120 W, 1/40 W/GOPS
C_{PU}, C_S	3600 \$, 30 \$
β, τ, γ	1.75 W/year, 20 years, 1
B (B_{Ref})	100 MHz (20 MHz)
$A \times L$ ($A_{\text{Ref}} \times L_{\text{Ref}}$)	32 × 8 (2 × 2) [11]
N_{SC}, N_{sym}	12, 14 [11]
N_{IQ}, N_{CPRI}, N_{LLR}	32, 32, 8 bits [11]
Ω_{IP}–Ω_{eCPRI}	1.02–1.10

Thus, the total power cost is given by the following equation:

$$E = \tau\beta(P + H_s + H_d) \tag{25}$$

E. Objective Function

The objective is to minimize the TCO while satisfying the model's constraints: $\min\ F_p + F_t + C_D + E$.

V. Numerical Results

To evaluate the proposed MILP model, we conducted a series of experiments to analyze the resulting network characteristics under different FS options. Our analysis focuses on fronthaul splits, therefore, we fix the DU-CU split to Option 2, which is recommended by both 3GPP and the O-RAN Alliance [12], [13]. For the RU–DU split, we consider Options 6, 7a, 7-2x, 7b, 7c, and 8, as these are the most commonly discussed in the literature. In particular, O-RAN has selected Option 7-2x as the reference split between the RU and DU [12].

For each configuration, we evaluate 50 independent network topologies, and all reported results correspond to averages over these realizations. The topologies are generated by randomly placing RUs, five candidate edge node locations, and a single cloud node over a 40×40 km^2 area. Splitter candidate positions are placed on a regular grid with 1 km spacing in both horizontal and vertical directions. The traffic load ρ of each RU is drawn from a uniform distribution in the range of 0.1 to 1 for each of the three considered timeslots, while RU power requirements are randomly selected as integer values in the interval $[5, 10]$ W.

The bandwidth requirements for each FS follow the formulations in Table I. The maximum allowable propagation delay is obtained by subtracting 50 μs from the corresponding latency constraint of each split, accounting for non-propagation delays. The remaining simulation parameters are summarized in Table II. The MILP model is solved utilizing the Python API of the Gurobi solver [14].

Fig. 2 shows the cost breakdown per RU for various RU counts. As expected, the cost per RU decreases as the network size increases due to the intensification of infrastructure sharing among the RUs, together with the increased concentration at the selected splitter positions, which in turn reduces fiber and trenching costs. For smaller networks, trenching dominates the overall cost, whereas fiber costs become increasingly significant as the number of RUs grows. This transition occurs because larger deployments allow multiple fibers to share the same trench, effectively diluting trenching expenses across a larger number of RUs. Other cost components, i.e, the installment, the distribution and the processing power contribute comparatively less to the total cost.

The results further show that Split 8 consistently leads to the highest cost across all scenarios, while Split 6 yields the lowest. In general, lower-layer splits result in higher per-RU costs, with the exception of Split 7-2x, which outperforms Split 7a. This behavior can be explained by two factors. First, as illustrated in Fig. 3, lower splits require a larger number PUs to be activated at the edge nodes. In particular, Split 8 activates approximately 2 PUs per RU, increasing both infrastructure and processing power costs. Second, lower splits impose higher bandwidth requirements, which reduce the number of RUs that can be aggregated per splitter, as shown in Fig. 4. Consequently, additional SM fiber cores are required between splitters and edge nodes, further increasing deployment costs. However, despite their higher cost, the potential to run lower fronthaul splits, such as Option 8, can be critical to enable ultra-low latency applications [15].

ILP and MILP formulations are often affected by scalability limitations, which can restrict their applicability to small-scale networks [5]. Nevertheless, Table III shows that the proposed model can be solved within a reasonable time even for larger deployments. Although the execution time for Split 7b exhibits noticeable increases at 300 and 500 RUs, it remains well below two hours in all evaluated scenarios. Since network planning problems can typically tolerate execution times on the order of hours or even days, these results indicate that the proposed MILP formulation is suitable for designing large-scale PWoF-enabled fronthaul networks.

TABLE III: Execution time in seconds for different number of RUs with 5 candidate edge nodes locations

Split	Number of RUs			
	100	200	300	500
6	158.55	299.72	463.15	767.98
7-2x	157.68	316.28	574.17	1834.56
7a	158.49	328.04	699.13	2095.01
7b	164.11	534.22	2115.12	5367.10
7c	153.82	307.60	485.75	817.69
8	151.35	298.73	466.06	980.87

VI. Conclusion

This work extends prior studies on fronthaul network design based on PWoF technology by explicitly incorporating the bandwidth, processing, and latency requirements imposed by different O-RAN FS options. We formulated the fronthaul

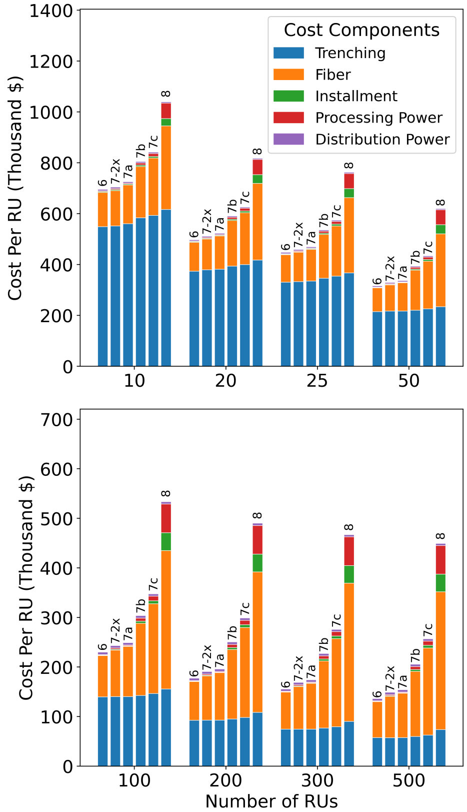

Fig. 2: Cost per RU for different numbers of RUs with 5 candidate edge node locations.

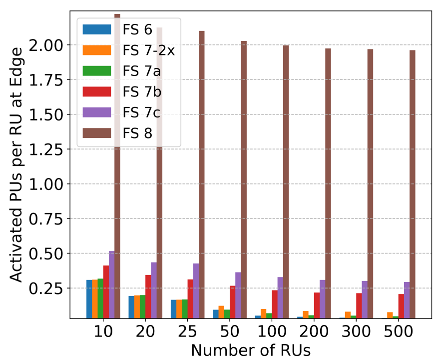

Fig. 3: Number of activated PUs at the edge nodes per RU for different numbers of RUs with 5 candidate edge node locations.

planning problem as an MILP model that optimizes network deployment while ensuring feasibility for any given FS configuration. Numerical results demonstrate that the proposed model can efficiently compute optimal solutions for networks with up to 500 RUs, indicating its potential applicability to even larger deployments. Overall, this study highlights the importance of taking into account FS in fronthaul design for 6G networks.

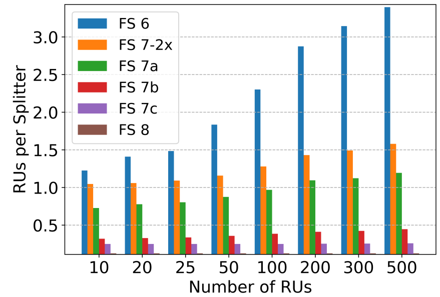

Fig. 4: Number of RUs per splitter for different number of RUs with 5 candidate edge node locations.

References

[1] P. Singh, A. Agarwal, and P. Kumar, "Navigating the 6g landscape: A systematic review of technology integration, implementation challenges, and strategic solutions," *Computer Networks*, vol. 272, p. 111663, 2025.

[2] M. Matsuura, "Power-over-fiber using double-clad fibers," *J. Lightwave Technol.*, vol. 40, pp. 3187–3196, May 2022.

[3] E. Erbayat, G. B. Figueiredo, S. Petale, S.-C. Lin, M. Matsuura, H. Hasegawa, and S. Subramaniam, "Toward scalable passive optically powered fronthaul networks," *Journal of Optical Communications and Networking*, vol. 17, no. 9, pp. D125–D136, 2025.

[4] E. Erbayat, G. B. Figueiredo, S.-C. Lin, M. Matsuura, H. Hasegawa, and S. Subramaniam, "Multi-DU fronthaul design leveraging power over fiber," in *2025 International Conference on Optical Network Design and Modeling (ONDM)*, 2025.

[5] E. Erbayat, L. G. S. Dos Santos, G. B. Figueiredo, S.-C. Lin, M. Matsuura, H. Hasegawa, and S. Subramaniam, "Latency-aware fronthaul network design using power-over-fiber," in *2025 25th Anniversary International Conference on Transparent Optical Networks (ICTON)*, pp. 1–4, 2025.

[6] E. Erbayat, G. B. Figueiredo, S.-C. Lin, M. Matsuura, H. Hasegawa, and S. Subramaniam, "Design of survivable fronthaul networks with power-over-fiber," in *2025 IEEE Future Networks World Forum (FNWF)*, pp. 1–6, IEEE, 2025.

[7] M. Masoudi, S. S. Lisi, and C. Cavdar, "Cost-effective migration toward virtualized C-RAN with scalable fronthaul design," *IEEE Systems Journal*, vol. 14, no. 4, pp. 5100–5110, 2020.

[8] M. S. Akhtar, J. Gupta, M. I. Alam, S. Majhi, and A. Adhya, "Fronthaul latency and capacity constrained cost-effective and energy-efficient 5g c-ran deployment," *Optical Fiber Technology*, vol. 80, p. 103392, 2023.

[9] Y. Yaguchi, Y. Miyakawa, S. Sugiura, S.-C. Lin, S. Subramaniam, H. Hasegawa, S. Fafard, D. Masson, and M. Matsuura, "Power-Over-Fiber Using a Pure-Silica Inner-Cladding Double-Clad Fiber and 976 nm Photovoltaic Power Converter for Improving Power Transmission Efficiency," in *50th European Conference on Optical Communications (ECOC 2024)*, vol. 2024, IET, 2024.

[10] S. Matoussi, I. Fajjari, N. Aitsaadi, and R. Langar, "User slicing scheme with functional split selection in 5g cloud-ran," in *2020 IEEE Wireless Communications and Networking Conference (WCNC)*, pp. 1–8, 2020.

[11] NTT DOCOMO, "R3-162102: CU-DU Split Refinement for Annex A." 3GPP TSG RAN WG3 Meeting #92, Document R3-162102, 2016. 3GPP Technical Specification Group Radio Access Network.

[12] O-RAN Alliance, "Control, User and Synchronization Plane Specification," Technical Specification O-RAN.WG4.CUS.0-v19.00, O-RAN Alliance e.V., Alfter, Germany, 2025. Work Group 4 (Open Fronthaul Interfaces WG).

[13] 3rd Generation Partnership Project (3GPP), "Study on new radio access technology: Radio access architecture and interfaces," Technical Report TR 38.801, 3rd Generation Partnership Project (3GPP), Mar. 2017. Version 14.0.0, Release 14.

[14] L. Gurobi Optimization, "Gurobi Optimizer Reference Manual," 2025.

[15] A. Larrañaga, S. Lagén, J. M. Fàbrega, J. M. Rivas-Moscoso, J. P. Fernández-Palacios, I. Tomkos, and R. Muñoz, "Fronthaul/midhaul networks: Capacity and latency requirements imposed by 6g disaggregated rans," *IEEE Communications Magazine*, vol. 63, no. 5, pp. 86–93, 2025.